POTSDAM-INSTITUT FÜR
KLIMAFOLGENFORSCHUNG

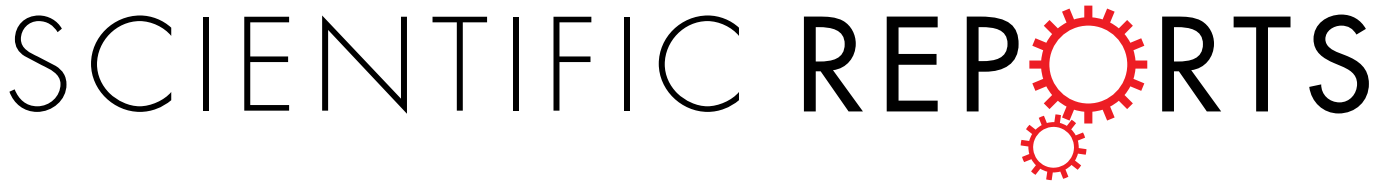

OPEN

Received: 14 August 2015
Accepted: 22 October 2015
Published: 24 November 2015

Experimental Study of the Triplet Synchronization of Coupled Nonidentical Mechanical Metronomes

Ji Jia[1], Zhiwen Song[1], Weiqing Liu[3], Jürgen Kurths[4,5,6,7] & Jinghua Xiao[1,2]

Triplet synchrony is an interesting state when the phases and the frequencies of three coupled oscillators fulfill the conditions of a triplet locking, whereas every pair of systems remains asynchronous. Experimental observation of triplet synchrony is firstly realized in three coupled nonidentical mechanical metronomes. A more direct method based on the phase diagram is proposed to observe and determine triplet synchronization. Our results show that the stable triplet synchrony is observed in several intervals of the parameter space. Moreover, the experimental results are verified according to the theoretical model of the coupled metronomes. The outcomes are useful to understand the inner regimes of collective dynamics in coupled oscillators.

Coupled dynamical systems which exhibit rich collective behavior are widely explored in biological[1,2], mechanical[3] or electrical, synthetic genetic networks[4]. With increasing strength of interactions between units, the whole coupled system may transit from some incoherent state to coherent ones, i.e. synchronization[5–7] and oscillation death[8,9]. Based on the specific form of the coherent motion, various types of synchronization, including complete synchronization[5], phase synchronization[6], partial phase synchronization[7], etc, are revealed in coupled oscillators. Since synchronization is one of the inner regimes of collective dynamics and pattern formation[10–12], it remains a topic of interest in numerous theoretical and experimental studies and finds various applications.

Among, phase synchronization, defined as the locking of phases between interacting oscillators with different natural frequencies, is strongly relevant to practical situation. Simply, two interacting oscillators are deemed to be n:m phase synchronization if the following condition is fulfilled for t is larger than a transient time T.

$$|n\varphi_1(t) - m\varphi_2(t)| < C, \tag{1}$$

where n and m are some integers and C is a rather small constant. Analyzing complex synchronization patterns in multi-frequency systems have been deeply applied in various fields, especially widely in biological systems such as the interaction of respiratory, cardiac and brain activities[13]. When considering a large number of interacting oscillators with complex interacting network structure and random natural frequency distribution, there are rich dynamics and patterns in the processes that the coupled system

[1]School of Science, Beijing University of Posts and Telecommunications, Beijing 100876, China. [2]State Key Lab of Information Photonics and Optical Communications, Beijing University of Posts and Telecommunications, Beijing 100876, China. [3]School of Science, Jiangxi University of Science and Technology, Ganzhou 341000, China. [4]Institute of Physics, Humboldt University Berlin, Berlin D-12489, Germany. [5]Potsdam Institute for Climate Impact Research, Telegraphenberg, Potsdam D-14415, Germany. [6]University of Aberdeen, Institute for Complex Systems and Mathematical Biology, Aberdeen, AB24 3UE, United Kingdom. [7]Nizhny Novgorod State University, Department of Control Theory, Nizhny Novgorod, 606950, Russia. Correspondence and requests for materials should be addressed to J.X. (email: Jhxiao@bupt.edu.cn) or W.L. (email: Wqliujx@gmail.com)

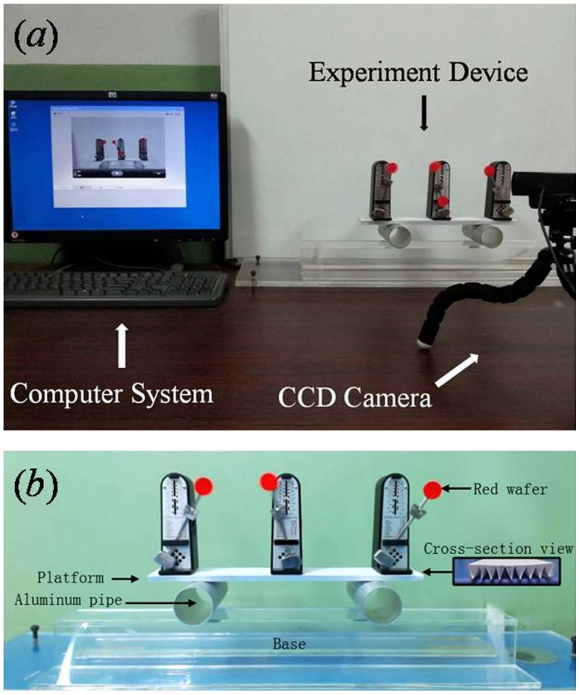

Figure 1. Experimental set up. (**a**) An overall view of the experimental system, including experiment device, CCD camera and computer system. (**b**) Front view of the experimental system recorded by the CCD camera, including the base, aluminum pipes, coupling board and metronomes. Several red wafers are pasted to mark the positions of desired parts.

transits from incoherent states to full phase locking states with increasing coupling interactions. Before reaching full phase locking state (any pair of coupling units satisfy the phase locking condition), the system may become a partial phase synchronization regime[7], i.e. some pairs or groups of oscillators are phase locked while others are not which forms several synchronous clusters. To reveal all synchronous states of a network efficiently, Kralemann *et al.*[14] defined a synchronous index to detect a triplet synchronization which is realized when *triplets* of interacting oscillators adjust their phases and frequencies so that the following conditions are fulfilled for t is larger than a transient time T,

$$|n\varphi_1(t) + m\varphi_2(t) + l\varphi_3(t)| < C, \tag{2}$$

where the integers n, m, l can be both positive and negative and C is a small constant. However in parallel, the conditions of the pair-wise synchrony equation (1) may *not* be satisfied for any pair of units. Although, triplet synchronization is theoretically predicted and detected in oscillator networks from observed data, it is expected to reveal various pattern formations of coupled oscillators and to contribute to research in neuroscience based on the binding by-synchrony hypothesis[15]. To our best knowledge, no experimental observation on triplet synchronization has been observed so far. Experimental discussion on the triplet synchronization is important for various applications, such as the interaction of different brain regions, where oscillations with a hierarchy of frequencies are ubiquitous.

Coupled pendulums are deemed as a paradigmatic model of exploring the dynamics of coupled systems since the pioneering work of Huygens. Recently, many scientific teams carried out a variety of experimental research work, such as Wu Ye *et al.*[16] showed a relationship theoretically and experimentally between the initial values and the friction damping force and the stable synchronous states of coupled metronomes system. Oliveira *et al.*[17] experimentally explored Huygens synchronization in two clocks hanging from an aluminum rail fixed to a masonry wall. Hu *et al.*[18] studied the synchronous behavior of three coupled metronomes, discovering a variety of synchronous states and the envelope synchronization phenomenon. Martens *et al.* found Chimera states in coupled metronome systems[19], etc[20,21]. Therefore, coupled pendulums are a promising candidate to observe triplet synchronization experimentally. We set up here a coupled system with three globally coupled pendulums and apply the synchronous index defined in Eq. (2) to observe the triplet synchronization.

In this article, we try to experimentally observe the triplet synchrony with the aid of the synchronous index. A model based on our experimental setup is built and analyzed to verify our experimental results.

Experimental setup

Figure 1 shows the experiment platform which consists of three metronome units supported by a piece of folded A4 paper on two aluminum pipes, a CCD (Charge Coupled Device) acquisition system connected to a computer and software of LABVIEW. The metronomes in our experimental work are all the Taktell Piccolino (Series 890) manufactured by Wittner GmbH & Co.KG in Germany. In order to improve the accuracy and simplicity, the latest experimental system are ameliorated based on the previous system[18–23]. An organic glass base of hollow cuboids shape is used to ensure that the system will not produce deformation because of its own weight. Two aluminum pipes (with 39 mm inside diameter, 41 mm outside diameter, and 100 mm length) are put on and perpendicular to the base. The aluminum pipes have a lot of advantages, such as that their rolling friction and shape hardly change and they have lighter mass.

Since the total energy supplied by the metronome units is limited (last about 20 minutes), it is difficult to realize synchronization if the coupling strength is not sufficient large. In order to enhance the effect of coupling, the crux of the problem is to provide more energy or reduce unnecessary loss. Without changing the structure of metronome, a paper-made platform was applied to substitute the coupling board used in the previous works[16,18]. A few pieces of A4 paper are folded as undulating shape so that it is strong enough to support the metronomes. Thus, with the lightness of the coupling board, the energy of the system will not waste too much of the kinetic energy of the coupling board. As a result, the coupling strength is guaranteed strong enough to realize synchronization between metronomes on the coupling board.

Three metronomes are put on the coupling board and a red wafer is pasted at the end of each pendulum and on the coupling board to improve the accuracy of recognition for the CCD camera. Then the motion of the pendulums and the coupling board can be conveniently recorded by tracing the center of the red wafers. In order to get accurate data, a camera with a high frame rate is set up by which one can record videos with a resolution of 720p (1280*720 pixels) and a frame rate of 30 frames per second. The time series of the pendulum of each metronome are recorded by handling the videos.

In our experiments, the metronomes are numbered as 1 to 3 from left to right. By adjusting the equivalent lengths of pendulums, we may change the frequency of the metronome slightly. (Noted that there are some slight differences between the actual frequencies and the set values which are caused by the instrumental errors (about 0.4%) in the mechanical structure of the metronomes. Therefore, we use all measured values of frequencies other than nominal ones of the metronome).

To provide enough energy necessary for the coupling, we set a relatively high value of initial frequency of metronomes as f_1=160 beats per minute (BPM) and f_1=176 BPM, while adjusting the value of the initial frequency f_3 of the 3rd metronome from 120 BPM to 200 BPM and so 107 values of f_3 are obtained. The time series for each initial frequency constellation are collected by the CCD camera, and the corresponding phases are calculated with the aid of a computer.

Analysis Methods

The synchronous ratio and order parameter are both effective indicators verifying the synchronous behavior of system. In the work of Kralemann *et al.*[14], the two indicators were combined and a special synchronous index was proposed as shown in Eq. (3) and (4). The pair-wise synchronization indices can be described as follows when two oscillators i and j are coupled:

$$\gamma_{n,m}^{(i,j)} = |<\gamma_{n,m}^{(i,j)}(t)>|,\ \gamma_{n,m}^{(i,j)}(t) = e^{i(n\varphi_i(t)+m\varphi_j(t))},\ i \neq j, \tag{3}$$

where $\varphi_i(t)$, $\varphi_j(t)$ are the phases of the oscillators i and j respectively, n and m are integers, and $<>$ is average on the time t. The oscillators i and j are considered as being n:m synchronized when the value of the pair-wise synchronization index $\gamma_{n,m}^{(i,j)}$ is equal to 1. Accordingly, when all three oscillators are coupled, the triplet synchronization indices can be calculated by equation (4):

$$\gamma_{n,m,l} = |<\gamma_{n,m,l}(t)>|,\ \gamma_{n,m,l}(t) = e^{i(n\varphi_1(t)+m\varphi_2(t)+l\varphi_3(t))}, \tag{4}$$

where $\varphi_{1,2,3}(t)$ are the phases of the oscillators 1–3 respectively, n, m and l are integers and $<>$ is average on the time t. Then the triplet synchronization indices $\gamma_{n,m,l}$ can be calculated for all possible integers of n, m, l. The state of the coupled system can be determined as the following cases. (1) If both the triplet synchronization index $\gamma_{n,m,l}$ and all the pair-wise synchronization indices $\gamma_{n,m}^{(i,j)}$ are approaching to 1, the coupled system is in complete phase synchronization other than triplet synchronization. (2) If the triplet synchronization index $\gamma_{n,m,l}$ is approaching to 1, while the pairwise synchronization indices are small, the coupled system is in triplet synchronization. (3) If the triplet synchronization index $\gamma_{n,m,l}$ is equal to 0, at least two of the three phases are completely independent.

Experimental Results

According to the recorded data of the swing angle $\varphi_i(t)$ of the pendulums (the data is recorded after a transient time T = 300 seconds), we calculate all triplet and pair-wise synchronization indices for all m, n, $l \subset [-Z, Z]$ (with $Z=5$ in our experiment) and record the maximal value of the indices as

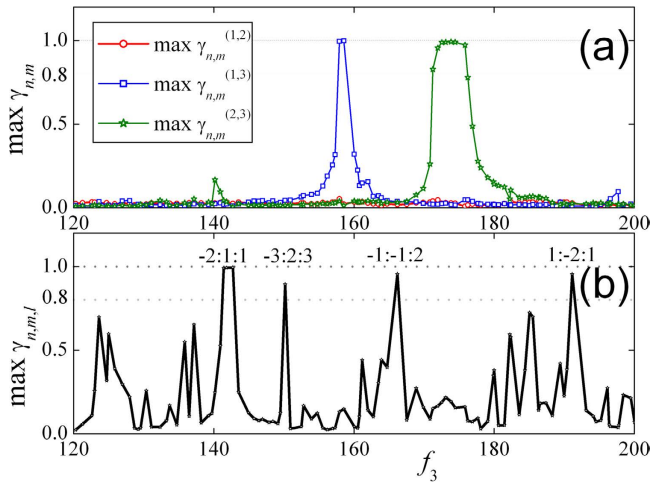

Figure 2. The distribution of synchronous indices in our experiments. (**a**) The distribution of the experimental pair-wise synchronous index in Eq. (3). The pair-wise synchronous indices between units 1, 2, 1, 3 and 2, 3, which are depicted as red, blue, and green line respectively, VS. the frequency f_3 of the 3rd metronome. (**b**) The triplet synchronous indices in Eq. (4) max$\gamma_{n,m,l}$ are shown as black line. The synchronous parameters n, m, l are labeled on the peaks of the corresponding frequencies.

max $\gamma_{n,m,l}$ or max $\gamma_{n,m}^{(i,j)}$. The maximal pair-wise synchronous indices between units (1, 2), (1, 3) and (2, 3) versus the frequency f_3 of the 3rd metronome are presented in Fig. 2(a), which are depicted as blue, red and green line respectively. For instance, when $f_3 = 158$ BPM or $f_3 = 176$ BPM, there are two intervals of $f_3 \in [158, 159]$ BPM and $f_3 \in [171, 176]$ BPM, where the pair-wise indices $\gamma_{1,1}^{(1,3)}$ and $\gamma_{1,1}^{(2,3)}$ are approx to 1 respectively. Therefore, the coupled system is in pair-wise synchronous state between (1, 3) and (2, 3) when $\gamma_{1,1}^{(1,3)}$ and $\gamma_{1,1}^{(2,3)}$ is larger than 0.8 as mentioned in ref. 14. In Fig. 2 (b), the maximal values of all triplet synchronous indices max $\gamma_{n,m,l}$ are shown as black line. It is obvious that there are four intervals of f_3 where max $\gamma_{n,m,l}$ is approaching 1, while the pair-wise indices of the corresponding intervals of f_3 are small (approaching zero). Therefore, the system reaches the triplet synchrony in those intervals of parameter f_3. That is to say, any pair of metronomes is asynchronous but the whole system of the three metronomes is in a triplet synchronous state when the parameter f_3 is in one of those four intervals. The corresponding integer parameters n, m, l are marked on the peaks of corresponding frequencies f_3.

Figure 3(a,b) present the time series of the swing angle $\phi_i(t)$ of the three metronomes when the coupled system is in a pair-wise synchronization and a triplet synchronous state respectively. It is difficult to figure out whether the pair-wise synchronization or the triplet synchronization is built between those three coupled metronomes only by the time series of the swing angles. However, if we calculate the values of $\gamma_{n,m}^{(i,j)}(t)$ and $\gamma_{n,m,l}(t)$ for a interval of time (8 seconds) respectively and dot them in the phase space of $\mathrm{Im}(\gamma_{n,m,l}(t))$ and $\mathrm{Re}(\gamma_{n,m,l}(t))$ (or $\mathrm{Im}(\gamma_{n,m}^{(i,j)}(t))$ and $\mathrm{Re}(\gamma_{n,m}^{(i,j)}(t))$), then the dots will distribute uniformly on a circle if no pair-wise synchronization (or triplet synchronization) is built, i.e., $\gamma_{n,m}$ (or $\gamma_{n,m,l}$) is small, otherwise, the dots are in a centralized distribution.

With the aid of the phase space representation of $\mathrm{Im}(\gamma_{n,m,l}(t))$ and $\mathrm{Re}(\gamma_{n,m,l}(t))$ (or $\mathrm{Im}(\gamma_{n,m}^{(i,j)}(t))$ and $\mathrm{Re}(\gamma_{n,m}^{(i,j)}(t))$), it is convenient to observe whether the coupled metronomes are in triplet or pair-wise synchronization. Figure 3(c–e) present the phase diagram of $\mathrm{Im}(\gamma_{n,m}^{(i,j)}(t))$ and $\mathrm{Re}(\gamma_{n,m}^{(i,j)}(t))$ for $(i, j) = (1, 2), (1, 3), (2, 3)$ respectively with $f_3 = 174.45$ BPM in experiment. The dots of $(\mathrm{Re}(\gamma_{n,m}^{(i,j)}(t)), \mathrm{Im}(\gamma_{n,m}^{(i,j)}(t)))$ for $(i, j) = (2, 3)$ distribute centrally on the circle, while those of $(i, j) = (1, 3)$ and $(1, 2)$ distribute uniformly on the circle. Therefore, pair-wise synchronization is only built between metronomes 2 and 3, which coincide well with the results presented in Fig. 2(a). However, the dots of $(\mathrm{Re}(\gamma_{n,m,l}(t)), \mathrm{Im}(\gamma_{n,m,l}(t)))$ are also distributed uniformly on the circle. Hence, there is no triplet synchronization between the coupled three metronomes, where the values of n, m, l are determined when the value of $\gamma_{n,m,l}$ is maximal. Meanwhile, we present the experimental results for $f_3 = 191.13$ BPM in Fig. 3 (g–j) which are corresponding to that in Fig. 3 (c–f). Obviously, there is no pair-wise synchronization but a triplet synchronization with $n{:}m{:}l = 1{:}-2{:}1$. What should be mentioned is that there are small amount of scatter dots in Fig. 3(e,j) which is caused by the sampling error of the CCD. As a result, the amount of data shown on the circle is limited (here we present data of 8 seconds) to observe the collective dynamics clear. To exhibit the collective dynamics more efficiently and without being influenced by the scatter dots caused by the sampling errors, the phase angle θ of the dot on the circle is

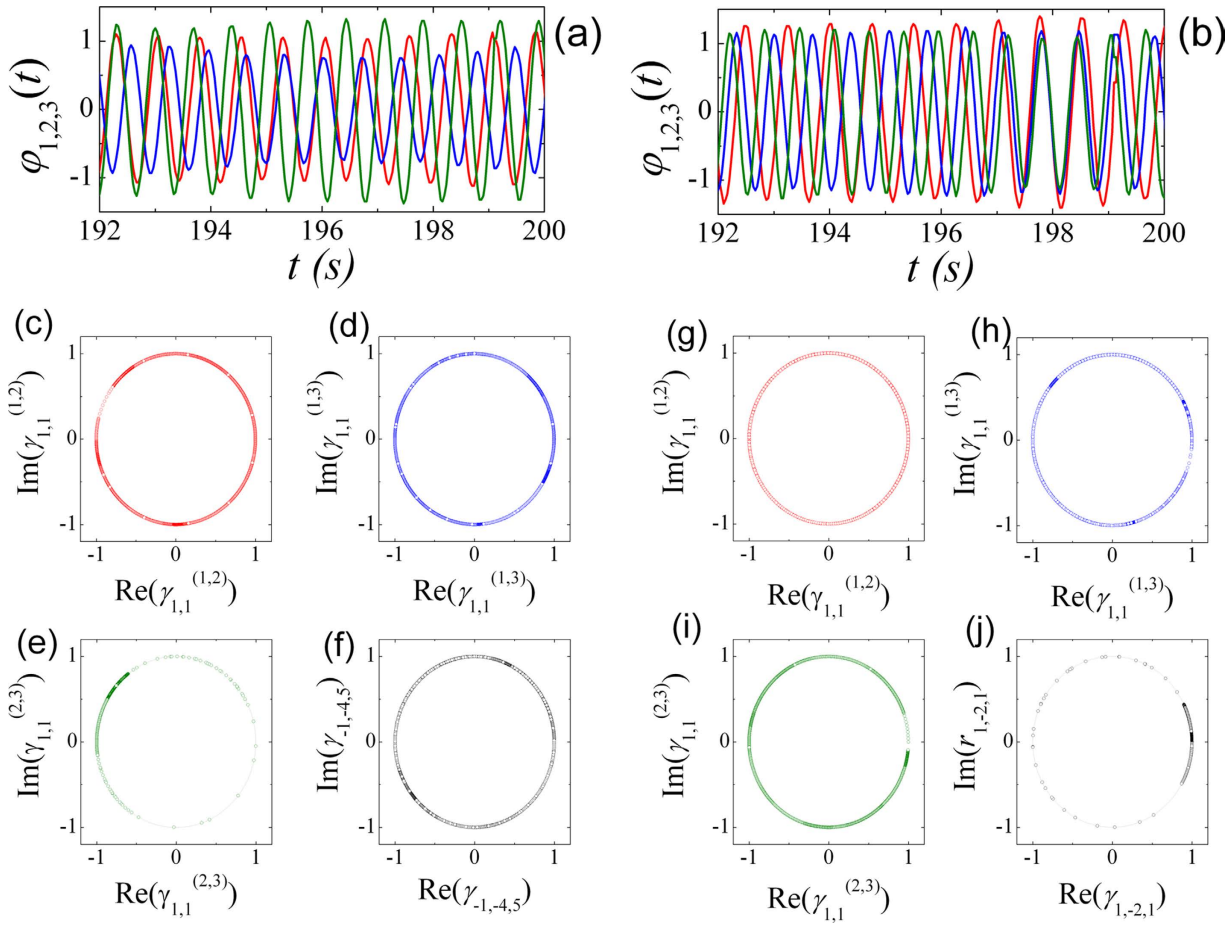

Figure 3. The time series of swing angle of three metronomes. The coupled system is in (**a**) pair-wise synchronization for $f_3 = 191.13$ BPM and (**b**) triplet synchronous state for $f_3 = 174.45$ BPM, respectively. (**c**–**e**) The phase diagram of $\mathrm{Im}(\gamma_{n,m}^{(i,j)}(t))$ and $\mathrm{Re}(\gamma_{n,m}^{(i,j)}(t))$ for $(i, j) = (1, 2), (1, 3), (2, 3)$ respectively, (**f**) the phase diagram of $\mathrm{Im}(\gamma_{n,m,l}(t))$ and $\mathrm{Re}(\gamma_{n,m,l}(t))$ for a period of 8 seconds as shown in (**a**). (**g**–**i**) The phase diagram of $\mathrm{Im}(\gamma_{n,m}^{(i,j)}(t))$ and $\mathrm{Re}(\gamma_{n,m}^{(i,j)}(t))$, (**j**) the phase diagram of $\mathrm{Im}(\gamma_{n,m,l}(t))$ and $\mathrm{Re}(\gamma_{n,m,l}(t))$ with $n{:}m{:}l = 1{:}-2{:}1$, for a period of 8 seconds as shown in (**b**).

defined as $\theta(t) = a\ \cos\left(\frac{\mathrm{Im}(\gamma_{n,m}^{i,j}(t))}{|\gamma_{n,m}^{i,j}(t)|}\right) + u^*\pi$, with $u = 0$ if $\mathrm{Re}(\gamma_{n,m}^{i,j}(t)) \geq 0$ and $u = 1$ otherwise. The phase locking can be judged according to the curve of the possibility density $P(\theta)$ of corresponding $\gamma_{n,m}^{i,j}(t)$. If the coupled system is in phase locking then the curve of corresponding $P(\theta)$ has a peak otherwise it will be uniformly distributed. Obviously, there is a peak of $P(\theta)$ around $\theta = \pi$ for $\gamma_{1,1}^{(2,3)}$ and a uniform distribution of $P(\theta)$ for $\gamma_{1,-4,5}$, $\gamma_{1,1}^{(1,2)}$, $\gamma_{1,1}^{(1,3)}$ as shown in Fig. 4 (a) when the coupled system is in pair-wise synchronization as Fig. 3(a). However, there is uniform distribution of $P(\theta)$ for $\gamma_{1,1}^{(2,3)}$, $\gamma_{1,1}^{(1,2)}$, $\gamma_{1,1}^{(1,3)}$, and peaks of $P(\theta)$ around $\theta = 0, \pi$ for $\gamma_{1,-2,1}$ as shown in Fig. 4 (b) when the coupled system is in triplet synchronization as Fig. 3(b).

Theoretical model and numerical results. To reveal the observed triplet synchronization in the experimental setup, a theoretical model derived from the experimental devices is analyzed[24,25]. The experimental devices are abstracted from that in refs 26–29 as shown in Fig. 5 where several pendulums with the same mass are coupled through a board, which can move horizontally. All pendulums are swinging around the fixed point above and in a common upright plane. The length and swinging angles of pendulums are denoted by l_i and ϕ_i. Two aluminum pipes are set parallel under the coupling board and thus the board can move horizontally. The displacement of the board is denoted by x; c_x and k_x are damping and linear force respectively.

Without the damping and driving force, the Lagrange equation of the system is as follows:

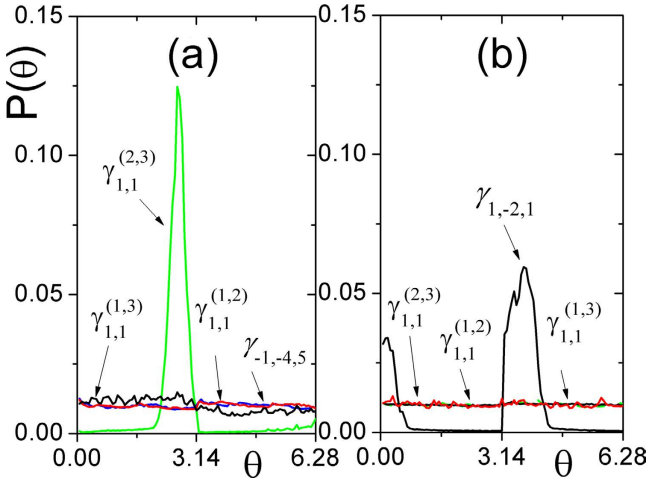

Figure 4. The phase distribution of the phase θ of **(a)** $\gamma_{1,1}^{(1,2)}$ (red line), $\gamma_{1,1}^{(1,3)}$ (black line), $\gamma_{1,1}^{(2,3)}$ (green line), $\gamma_{1,-4,5}$ (blue line) corresponding to Fig. 3(c–f), respectively. (b) $\gamma_{1,1}^{(1,2)}$ (red line), $\gamma_{1,1}^{(1,3)}$ (green line), $\gamma_{1,1}^{(2,3)}$ (blue line), $\gamma_{1,-2,1}$ (black line) corresponding to Fig. 3(g–j).

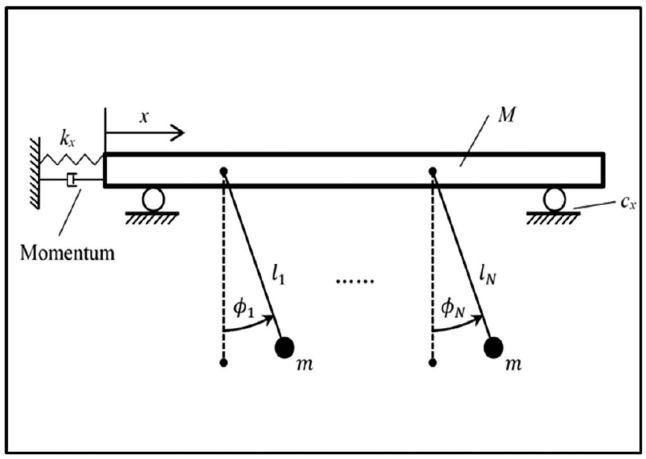

Figure 5. Theoretical model of coupled metronomes.

$$L = \frac{1}{2}M\dot{x}^2 + \sum_{i=1}^{N}\frac{m_i}{2}\left\{\left[\frac{d}{dt}(x + l_i \sin \phi_i)\right]^2 + \left[\frac{d}{dt}(l_i \cos \phi_i)\right]^2\right\} + \sum_{i=1}^{N} m_i g l_i \cos \phi_i - \frac{1}{2}k_x x^2, \tag{5}$$

and can be simplified into,

$$L = \frac{1}{2}\left(M + \sum_{i=1}^{N} m_i\right)\dot{x}^2 + \sum_{i=1}^{N}\left(m_i \dot{x} l_i \dot{\phi}_i \cos \phi_i + \frac{m_i}{2} l_i^2 \dot{\phi}_i^2 + m_i g l_i \cos \phi_i\right) - \frac{1}{2}k_x x^2, \tag{6}$$

where M is the mass of the board, $m_i = 1$ is the mass of the pendulum, x is the displacement of the board with $x(0) = 0$. l_i and ϕ_i are the length and angle of the ith pendulum, g is the gravity. We define the right direction as the positive direction. In Huygens experiments, the coupling board was limited by magnetic substance, and therefore the parameter k_x is remained to repeat the earlier work and it is set as $k_x = 0.5$.

With the effects of damping and driving force, which is caused by the escapement mechanism of the metronomes, the dynamic equation of the coupled system can be solved:

$$m_i l_i^2 \ddot{\phi}_i + m_i \ddot{x} l_i \cos \phi_i + c_{\phi_i}\dot{\phi}_i + m_i g l_i \sin \phi_i = M_D, \quad i = 1, 2, 3 \tag{7}$$

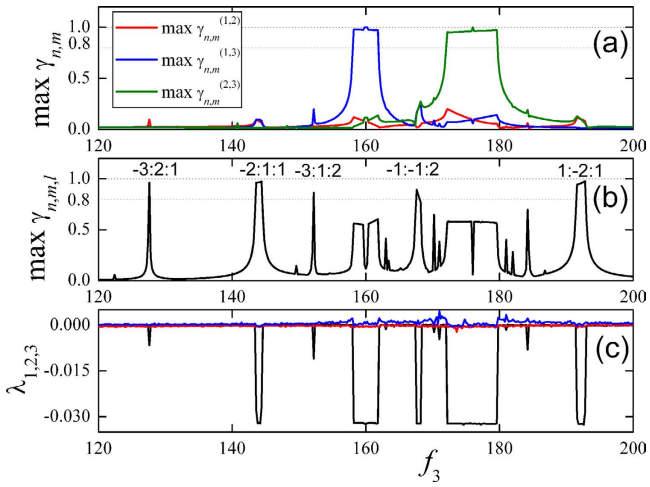

Figure 6. The distributions of synchronous indices in numerical simulation. (**a**) The distributions of pair-wise synchronous indices, and the max$\gamma_{n,m}^{(1,2)}$, $\gamma_{n,m}^{(1,3)}$ and $\gamma_{n,m}^{(2,3)}$ are plotted by red, blue and green curves respectively. There are two sections where the pairwise indices are greater, around the frequencies of $f_3 \approx 160$ BPM and $f_3 \approx 176$ BPM, and it shows that the metronomes (1, 3) or (2, 3) of the system are pair-wise synchronous respectively and synchronous parameters are $n = m = 1$. (**b**) The triplet synchronous indices, plotted by the black curve. There are 5 sections where max $\gamma_{n,m,l}$ is approaching 1 (larger than 0.8), i.e. the system reaches triplet synchrony, and the synchronous ratios are labeled on the peak of the corresponding frequencies. (**c**) The distribution of the largest three of Lyapunov exponents. When the third largest Lyapunov exponent λ_3 is negative, the system is phase-locked.

$$\left(M + \sum_{i=1}^{3} m_i\right)\ddot{x} + c_x\dot{x} + k_x x + \sum_{i=1}^{3}(m_i l_i \ddot{\phi}_i \cos\phi_i - m_i l_i \dot{\phi}_i^2 \sin\phi_i) = 0, \tag{8}$$

where $i = 1, 2, 3$, $c_{\phi_i} = 0.01$ is the damping of each pendulum, and c_x is the damping of the coupling board. M_D is the driving force. When the rod of the pendulum swings cross zero and the angle is less than $\gamma_N = 5°$, the driving force is produced as follows:

$$M_{D_i} = \begin{cases} 0.075 m_i & 0 < \phi_i < \gamma_N, \quad \dot{\phi}_i > 0 \\ -0.075 m_i & -\gamma_N < \phi_i < 0, \quad \dot{\phi}_i < 0, \\ 0 & otherwise \end{cases} \tag{9}$$

The fourth order Runge-Kutta method is applied and the interval time is set as $\Delta t = 0.001$ in our simulations. Exceptionally, setting $\Delta t = 0.0001$ is helpful to solve the problems about Lyapunov exponent. At the time $t = 0$, the initial velocities of all objects and displacement of the coupling board are set as zero, and the initial values of the swinging angles are set randomly. The coupled system will go into stable states usually after 300 seconds of transient time.

While simulating equations (7) and (8) numerically, we fix the parameters as follows, $m_i = 1.0$, $\gamma_N = \pi/36$, $\dot{\phi}_1 = \dot{\phi}_2 = 0$, $x = \dot{x} = 0$, $M = 30$ and $c_{\phi_i} = 0.01$. In order to compare them with our experimental results, we firstly fix the frequencies of two metronomes as f_1=160 BPM and f_1=176 BPM, and adjust f_3 from 120 to 200 BPM gradually. The length of the pendulum can be determined according to the equation of $l_i \approx g\,(60/\pi f_i)^2$. Then the pair-wise synchronous indices and the triplet synchronous indices can be calculated respectively according to the recorded time series of $\phi_{1,2,3}$. The total time of the recorded time series of phase are 500 seconds after a transient time $T = 300$ seconds. The results are not concerned with the length of the time interval. For example, the results of 2000 seconds and of 5000 seconds are the same as that of 500 seconds. For each value of f_3, we determine the maximal synchronous index among all possible sets of n, m (or n, m, l) in a range of [−Z, Z] with Z = 5. If the value of max $\gamma_{n,m,l} > 0.8$, and the maximal value of $\gamma_{m,n}$ is small, then that triplet synchronization is built up between the coupled metronomes. Figure 6(a) shows the distributions of pair-wise synchronous indices, and the max$\gamma_{n,m}^{(1,2)}$, $\gamma_{n,m}^{(1,3)}$ and $\gamma_{n,m}^{(2,3)}$ are plotted by red, blue and green curves respectively. There are two intervals of parameter f_3 where the pair-wise indices are approaching to 1, around the frequencies of $f_3 \approx 160$ BPM and $f_3 \approx 176$ BPM. Therefore, the metronomes (1, 3) or (2, 3) of coupled system are in a pair-wise synchronous state respectively with the synchronous parameters $n = m = 1$. Accordingly,

the maximal value of triplet synchronous indices are presented in Fig. 6(b) and plotted by black curve. There are 5 intervals of f_3 where max $\gamma_{n,m,l} > 0.8$, with the parameters n,m,l as marked on the corresponding intervals (such as −2:1:1 indicates that the synchronous parameters are $n = -2, m = 1, l = 1$ which realize the maximal value of the triplet index for given f_3). However, the n:m pair-wise synchronous are excluded only in the range of [−Z, Z] with Z = 5 for the sake of consistent with the experimental one. It is necessary to exclude higher order of n:m pair-wise synchronous. Therefore, we calculate and record the maxima of the pairwise synchronous index for all possible n:m in the interval of [−100, 100] with parameter f_3 being in stage when the the maximal value of the triplet indices are above 0.8. The maximal pairwise synchronous index is $\gamma^{(1,3)}_{(95,-75)} = 0.41$ which is less than 0.8. Even larger range of n, m, for example, [−300, 300], the maximal pairwise synchronous indices are not larger than those when m and n are in the range of [−100, 100]. Therefore, we may deduced that triplet synchronization is stable for given range of m and n. However, it is a time-consuming work for even larger range of n, m.

The largest three Lyapunov exponents are an effectively indicator of phase synchronization between the coupled system. Since the metronome is a mechanical system which is driven by discontinuous force from a spring, the standard algorithm does not work for the discontinuous dynamical equation. Thus the largest three of them, $\lambda_{1,2,3}$, are calculated based on the algorithm introduced in refs 30,31. To exclude the effects of statistical fluctuation, 20000 seconds of time series are recorded to calculate the Lyapunov exponents. The Lyapunov exponents are stable when the time increases from 10000 seconds to 20000 seconds. In Fig. 6 (c), the largest three Lyapunov exponents are presented for different values of f_3. Phase synchronization is characterized by a negative value of the third largest Lyapunov exponent λ_3. In the intervals of triplet or pair-wise synchrony, two of the largest three exponents are zero and the other one is negative and it shows that the system is quasi-periodic at these moments. In other frequencies, none of the three exponents are negative and at least two of them are approaching to zero, so the system is in high dimensional quasi-periodic or chaotic state.

To compare the numerical results with the experimental ones, we recorded the time series of the coupled metronomes' angle for $f_3 = 192$ BPM and $f_3 = 1752$ BPM, respectively. We also cannot determine whether the coupled system is in triplet or pair-wise synchrony only from the time series. However, the phase space diagram of $\mathrm{Im}(\gamma_{n,m,l}(t))$ and $\mathrm{Re}(\gamma_{n,m,l}(t))$ (or $\mathrm{Im}(\gamma^{(i,j)}_{n,m}(t))$ and $\mathrm{Re}(\gamma^{(i,j)}_{n,m}(t))$) present clear relationships between the coupled metronomes. Obviously, when the value $f_3 = 192$ BPM, pair-wise synchronization is built between metronomes 2 and 3, since the dots are collected in a small range on the circle as shown in Fig. 7(e). However, there is no triplet synchronization between the three coupled metronomes, since the dots are distribute uniformly on the circle as shown in Fig. 7(f) when *n, m, l* has value (−1:5:−4) when $\gamma_{n,m,l}$ is maximal. When the value $f_3 = 175$ BPM, there is no pair-wise synchronization between the metronomes 1,2, 1,3, and 2,3, since the dots distribute uniformly on the circle as shown in Fig. 7(g–i). However, triplet synchronization with *n:m:l* = 1:−2:1 is built between them as shown in Fig. 7(j).

Another approach to verify the motion states is via Poincare maps which are got by recording the values of ϕ_1 and ϕ_2 when $\phi_3 = 0$ as shown in Fig. 8. The Poincare map (in Fig. 8(a), $f_3 = 175$ BPM) is a horizontal line with small variation in the parameter space of ϕ_1 versus ϕ_2 when $\phi_3 = 0$. Hence, it is confirmed this way that the coupled system built pair-wise synchronization only between metronomes 2 and 3 while there is no pair-wise synchronous between ϕ_1 and ϕ_2. As a result, ϕ_1 influences the pair-wise synchronization between ϕ_2 and ϕ_3 which leads to a small modulation or perturbation. However, the Poincare map (in Fig. 8(b) $f_3 = 175$ BPM) shows that both phases ϕ_1 and ϕ_2 vary from zero to 2π and remain in a functional relationship $|n\phi_1(t) + m\phi_2(t)| < C$ with $n:m = 1:-2$ when $\phi_3 = 0$. Hence, there is no pair-wise synchronization between ϕ_2 and ϕ_3, ϕ_1 and ϕ_3 according to the fact that ϕ_1 and ϕ_2 vary from zero to 2π when $\phi_3 = 0$. If the coupled metronome system is triplet synchronous with *n:m:l* = 1:−2:1, then $|n\phi_1(t) + m\phi_2(t) + l\phi_3(t)| < C$. If $\phi_3 = 0$, it comes to the result of $|n\phi_1(t) + m\phi_2(t)| < C$ with $n:m = 1:-2$ as shown the Poincare map in Fig. 8(b).

Comparing Figs 2 and 6, it is obvious that the numerical analyses are consistent with our experimental results and the theoretical model is effective to describe the experimental process. However, it should be mentioned that there are some differences between them. Firstly, there are 5 intervals of triplet synchrony, in numerical results but only 4 of them are observed in our experiments. By checking our experimental results carefully, we find that there is a smaller peak at the frequency of $f_3 = 125$ BPM, and its maximum value is less than 0.8. Next, the sections of pair-wise synchrony, which are observed in our experiments, are smaller than the simulated ones, especially at the frequency of $f_3 \approx 160$ BPM. A reasonable explanation is that the interval of adjacent frequencies cannot be adjusted as small enough as the width of the peak in the experiments, thus the exact values of f_3 corresponding to the peak of the index cannot be observed. This can be explained as that the results are almost the same when f_3 is larger, but the synchronous sections are much more narrow in the experiments when f_3 is smaller. A possible reason is, due to the escapement mechanism of the metronomes, that the lower frequencies cause less energy in unit time and the coupling effect is decreased. To verify the reason of the difference as described above and explore the universal rule of this behavior, the distributions of more extensive and various parameter spaces are discussed.

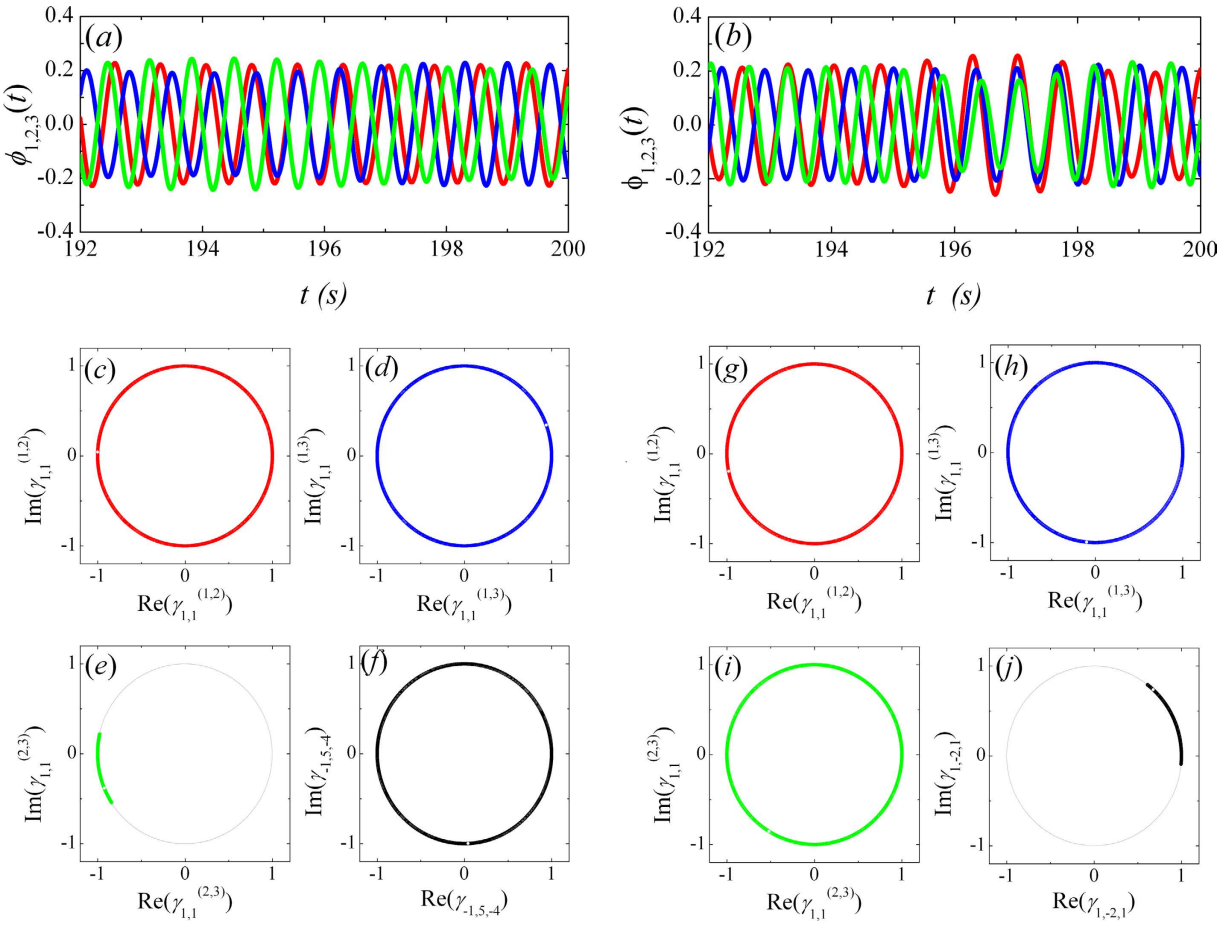

Figure 7. Numerical results of the time series of metronomes' swing angles. The coupled system is in (**a**) pair-wise synchronization for $f_3 = 192$ BPM and (**b**) triplet synchronous state for $f_3 = 175$ BPM, respectively. (**c–e**) The phase diagram of $\mathrm{Im}(\gamma_{n,m}^{(i,j)}(t))$ and $\mathrm{Re}(\gamma_{n,m}^{(i,j)}(t))$ for $(i, j) = (1, 2), (1, 3), (2, 3)$ respectively, (**f**) the phase diagram of $\mathrm{Im}(\gamma_{n,m,l}(t))$ and $\mathrm{Re}(\gamma_{n,m,l}(t))$ with $n{:}m{:}l = -1{:}5{:}-4$ for a period of $t = 192 - 200$ s as shown in (**a**). (**g–i**) The phase diagram of $\mathrm{Im}(\gamma_{n,m}^{(i,j)}(t))$ and $\mathrm{Re}(\gamma_{n,m}^{(i,j)}(t))$, (**j**) the phase diagram of $\mathrm{Im}(\gamma_{n,m,l}(t))$ and $\mathrm{Re}(\gamma_{n,m,l}(t))$ with $n{:}m{:}l = 1{:}-2{:}1$, for a period of $t = 192-200$ s as shown in (**b**).

Since the mass of the coupling board affects the strength of the coupling, it is necessary to investigate the effect of the mass of the coupling board on the synchronous index. As shown in Fig. 9(a), the ordinate denotes M, the mass of the board, and the abscissa denote f_3, the frequency of the 3rd metronome. We find that the system shows extremely complex phenomena when the mass is small. With the increasing of the mass, only a few sections are maintained. When the mass is about 30, system will work as our theoretical analysis predicts. The frequency difference Δf is fixed as $\Delta f = f_2 - f_1 = 16$ BPM, as shown in Fig. 9(b) (the ordinate denotes f_2), and third one will influence the synchronous index. In addition, if the frequency of the 1st metronome is fixed as $f_1 = 160$ BPM, we observe a relationship between f_2 and f_3 in Fig. 9(c).

Therefore, the distribution of the synchronous index is related to the frequencies of all metronomes. When the frequency differences are large enough, the behavior of the system depends on the coupling strength. We set the parameters in order to make the phenomena more clear and intuitive.

Let us consider the synchronization indices based on the parameter spaces of f_2 and f_3 by fixing the value of $f_1 = 160$ BPM. The results indicate that there are rich dynamics as the complete synchronization (white area), the triplet synchrony (black area), the pairwise synchrony (wine area) and unlocked states (light gray area) as shown in Fig. 10. Obviously, the probability for triplet synchrony is the smallest in the parameter spaces of f_2 and f_3.

To sum up, it is obviously that a very tiny difference in the value of parameters in the model system may lead to a deviation from the synchronization states. In consequence, taking inevitable instrumental error into account, the numerical analyses can be considered to be consistent with our experimental results as well as in the theoretical model. Based on the method of synchronous index, the triplet synchrony is observed in the experimental system of coupled metronomes.

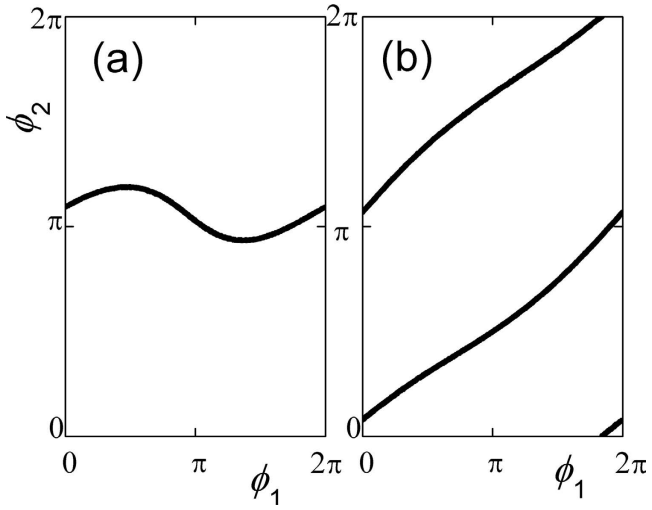

Figure 8. A Poincare map of system Eq. (7) (8). (a) For fixing $\phi_3 = 0$ and f_3=175 BPM, ϕ_2 keeps constantly with small fluctuation as ϕ_1 increases. There is pairwise synchronization between metronomes 2 and 3 while without pairwise synchronization between metronomes 1 and 2. (**b**) For fixing $\phi_3 = 0$ and f_3=192 BPM, both ϕ_1 and ϕ_2 keep increasing from zero to 2π simultaneously, remaining, however, in a functional relationship $|n\phi_1(t) + m\phi_2(t)| < C$ with $n{:}m = 1{:}-2$, this is an example of a triplet-synchronous state.

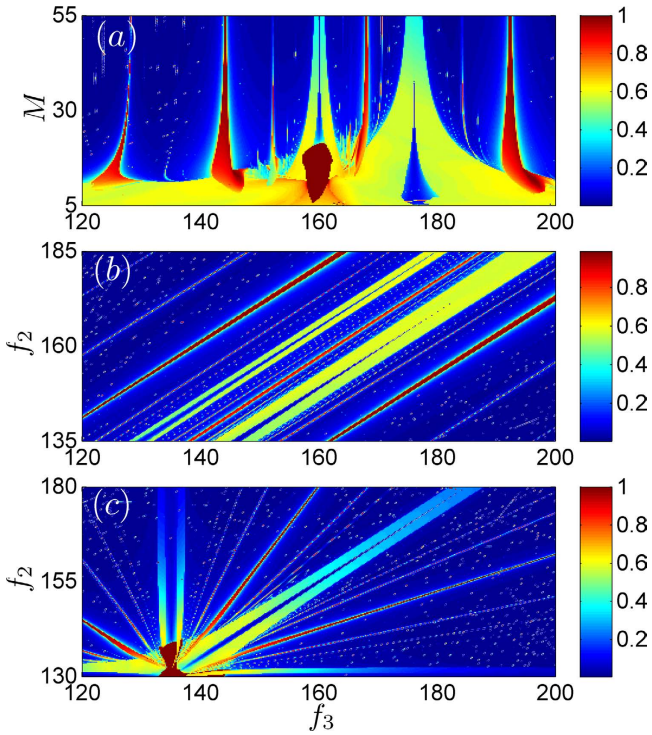

Figure 9. The parameter spaces of the synchronous indices Eq. (4) of system Eq. (8). The different colors denote the value of indices. (**a**) The effect of the mass of coupling board vs f_3, fixing f_1=160 BPM and f_1=176 BPM. (**b**) The effect of frequencies of the first two metronomes and the third one, by fixing $\Delta f = f_2 - f_1 = 16$ BPM. (**c**) The effect of the frequencies of the 2nd and 3rd metronomes, by fixing f_1=160 BPM.

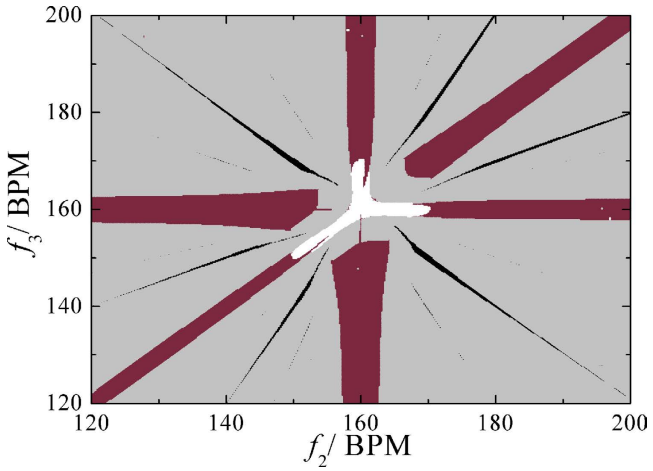

Figure 10. The distribution of synchronous index of system in the frequency space. When f_1=160 BPM, white areas denote the complete synchronization of system, black ones denote the triplet synchronization. Wine ones denote the pair-wise synchrony and light gray ones are unlocked states.

Discussion

In this paper, according to the theory of synchronization, an oscillation system of coupled metronomes was set up and triplet synchrony is discovered in a real experiment. By establishing the theoretical model and simulating the system numerically, we obtain consistent findings in experiments as well as theoretical models. By expanding the parameter spaces, we uncover more abundant nonlinear dynamic behaviors of coupled metronomes. It has been validated that the method of synchronous index is a useful tool to study experimental systems. Moreover, we propose a more direct method to determine triplet synchronization and pair-wise synchronization by a phase space representation of $\mathrm{Im}(\gamma_{n,m,l}(t))$ and $\mathrm{Re}(\gamma_{n,m,l}(t))$ (or $\mathrm{Im}(\gamma_{n,m}^{(i,j)}(t))$ and $\mathrm{Re}(\gamma_{n,m}^{(i,j)}(t))$). This approach can be used as a basis for applications and to detect such synchronization in various fields such as engineering, neuroscience, biology, etc. The discovery of triplet synchrony in our experimental system will help us to explore the physical mechanism of complex synchronization patterns in other real systems as well. It is hoped to play a role of guidance and construction in complicated synchronization behaviors in future.

Methods

Experiments. For the convenience of CCD acquisition, the bobs of the pendulums are pasted with red wafers respectively. The model of the metronome is Series 890 by DE Taktell with a mass (94 g). Its energy is supplied by a hand wound spring. The frequency of the metronome can be adjusted by changing the position of the mass on the pendulum bob, which denotes that the equivalent pendulum length is changed. The standard settings of the metronome's frequency range from 40 ticks per minute (largo) to 208 ticks per minute (prestissimo), but not limited to the scale. The supporting folded A4 paper is light (4.366 g), since the pendulum bob's swing direction is perpendicular to the aluminum pipes axes, a bidirectional coupling between the metronomes is generated via the folded paper, which has a tuning impact on the metronomes. Two parallel aluminum pipes (with inner (external) diameter 39 mm (41 mm)) support the folded A4 paper. Under the aluminum pipes there is a horizontal adjustment equipment.

Simulations. The equations (1) and (2) are solved by the 4th-order Runge-Kutta method with a time step of 0.0001. The following parameters remain unchanged in the next parts of numerical calculation. We fixed the parameters $m_1 = m_2 = 1.0$, $\gamma_N = \pi/36$, $\dot{\phi}_1 = \dot{\phi}_2 = 0$, $x = \dot{x} = 0$, $M = 30$ (calculated according to the experimental data) and $c_{\phi_i} = 0.01$.

References

1. Strogatz, H. H. & Stewart, I. Coupled oscillators and biological synchronization. *Sci. Am.* **269,** 102–109 (1993).
2. Strogatz, S. H. NobertWiener's brain waves *Lect. Notes Biomath.* **100,** 122–138 (1994).
3. Song, G., Buck, N. V. & Agrawal, B. N. Spacecraft Vibration Reduction Using Pulse-Width Pulse-Frequency Modulated Input Shaper. *Journal of Guidance, Control, and Dynamics* **22,** 433 (1999).
4. Ullner, E., Zaikin, A., Volkov, E. I. & Garcia-Ojalvo, J. Multistability and clustering in a population of synthetic genetic oscillators via phase-repulsive cell-to-cell communication. *Phys. Rev. Lett.* **99,** 148103 (2007).
5. Pecora, L. M. & Carroll, T. L. Synchronization in chaotic system. *J. Phys. Rev. Lett.* **64,** 821 (1990).
6. Rosenblum, M. G., Pikovsky, A. S. & Kurths, J. Phase synchronization of chaotic oscillators. *J. Phys. Rev. Lett.* **76,** 1804 (1996).
7. Schelter, B., Winterhalder, M., Dahlhaus, R., Kurths, J. & Timmer, J. Partial phase synchronization for multivariate synchronizing systems. *Phys. Rev. Lett.* **96,** 208103 (2006).

8. Zou, W. *et al.* Restoration of rhythmicity in diffusively coupled dynamical network, *Nature Communications* **6,** 7709 (2015).
9. Liu, W. *et al.* Oscillator death induced by amplitude-dependent coupling in repulsively coupled oscillators, *Phys. Rev. E* **91,** 052902 (2015).
10. He Z., Wang X., Zhang G. Y. & Zhan M. Control for a synchronization-desynchronization switch *Phys. Rev.E* **90,** 012909 (2014).
11. Liu P., Deng Z. , Yang L., Zhan M. & Wang X. Network approach to the pinning control of drift-wave turbulence, *Phys. Rev. E* **89,** 062918 (2014).
12. Fu C., Lin W., Huang L. & Wang X. Synchronization transition in networked chaotic oscillators: The viewpoint from partial synchronization, *Phys. Rev.E* **89,** 052908 (2014).
13. Musizza, B. *et al.* Interactions between cardiac, respiratory and EEG-δ oscillations in rats during anaesthesia. *The journal of Physiology* **580** (Pt 1), 315–326 (2007).
14. Kralemann, B., Pikovsky, A. & Rosenblum, M. Detecting triplet locking by triplet synchronization indices. *Phys. Rev. E* **87,** 052904 (2013).
15. Gray, C. M., Konig, P., Engel, A. K. & Singer, W. Oscillatory responses in cat visual cortex exhibit inter-columnar synchronization which reflects global stimulus properties. *Nature* **338,** 334 (1989).
16. Wu, Y., Wang, N. C., Li, L. X. & Xiao, J. H. Anti-phase synchronization of two coupled mechanical metronomes. *Chaos* **22,** 023146 (2012).
17. Oliveira H. M. & Melo L. V. Huygens synchronization of two clocks, *Sci. Rep*. **5** 11548 (2015).
18. Hu, Q., Liu, W., Yang, H., Xiao, J. & Qian, X. Experimental Study on Synchronization of Three Coupled Mechanical Metronomes. *Eur. J. Phys.* **34,** 391 (2013).
19. Martens, E. A., Thutupalli, S., Fourriere, A. & Hallatschek, O. Chimera states in mechanical oscillator networks. *Proc. Natl. Acad. Sci. USA* **110(26),** 10563–10567 (2013).
20. Boda, S., Ujvari, S., Tunyagi, A. & Neda, Z. Kuramoto-type phase transition with metronomes. *Eur. J. Phys.* **34,** 1451–1463 (2013).
21. Song, Z. W., Wu, Y., Liu, W. Q. & Xiao, J. H. Experimental Study of the Irrational Phase Synchronization of Coupled Nonidentical Mechanical Metronomes. *PLoS One* **10(3),** e0118986 (2015).
22. Kapitaniak, M., Czolczynski, K., Perlikowski, P., Stefanski, A. & Kapitaniak, T. Synchronization of clocks. *Phys. Rep*. **517,** 18 (2002).
23. Pantaleone, J. Synchronization of Metronomes. *Am. J. Phys*. **70,** 992–1000 (2002).
24. Zou, Y., Pazo, D., Romano, M. C., Thiel, M. & Kurths, J. Distinguishing quasiperiodic dynamics from chaos in short-time series. *Phys. Rev. E.* **76,** 016210 (2007).
25. Czolczynski, K. Huygens' odd sympathy experiment revisited. *Int. J. Bifurcat. Chaos* **21,** 2047 (2011).
26. Martens, E. A. Chimera states in mechanical oscillator networks. *Proc. Natl. Acad. Sci. USA* **110,** 10563–10567 (2013).
27. Czolczynski, K., Perlikowski, P., Stefanski, A. & Kapitaniak, T. Clustering of Huygens' clocks. *Prog. Theor. Phys*. **122,** 1027 (2009).
28. Ulrichs, H., Mann, A. & Parlitz, U. Synchronization and chaotic dynamics of coupled mechanical metronomes. *Chaos* **19,** 043120 (2009).
29. Perlikowski, P., Kapitaniak, M., Czolczynski, K., Stefanski, A. & Kapitaniak, T. Chaos in coupled clocks. *Int. J. Bifurcat. Chaos* **22,** 1250288 (2012).
30. Muller, P.C. Calculation of Lyapunov Exponents for Dynamic Systems with Discontinuities. *Chaos* **5,1671**–1681 (1995).
31. Hinrichs, N., Oestreich, M. & Popp, K. Dynamics of Oscillators with Impact and Friction. *Chaos* **8,535**–558 (1997).

Acknowledgements

This research recieved funds from the National Natural Science Foundation of China (Grant Nos. 61377067, 10575016, 11262006) and the Fundamental Research Funds for the Central Universities. W.L. was supported by the project of high school of Jiangxi province (Grant No. KJLD14047), and the training plan of young scientists of Jiangxi province.

Author Contributions

Conceived and designed the experiments: J.X., Z.S. and J.J. Performed the experiments: Z.S. and J.J. Analyzed the data: Z.S. and J.J. Contributed reagents/materials/analysis tools: Z.S., J.J., J.X. and W.L. Wrote the paper: Z.S., J.X., W.L. and J.K. All the authors discussed the results, drew conclusions and edited the manuscript.

Additional Information

Competing financial interests: The authors declare no competing financial interests.

How to cite this article: Jia, J. *et al.* Experimental Study of the Triplet Synchronization of Coupled Nonidentical Mechanical Metronomes. *Sci. Rep.* **5**, 17008; doi: 10.1038/srep17008 (2015).